Reconstructing the 3D Cardiac Shape by Using Magneto-Cardiography

[1]Ms.Gauravi Shetty, [2]Mr.Murugesh K
[1]M.Tech in Digital Electronics, [2]Assistant Professor,
[1]Department of ECE,
[1]Don Bosco Institute of Technology, Bangalore, India

***Abstract*—The three dimensional reconstruction of heart requires division process which uses additional imaging modalities, that is useful in clinical applications for the cardiovascular 3D perspective. In this way this paper recommends, following a 3D cardiovascular structure by making utilization of magneto-cardiography information without making utilization of further imaging procedures. The construction of heart structure was finished by two routines to be specific spatial filtering and coherence mapping. The force of cardiovascular movement is initially computed by AGMN-RUG(array gain constraint minimum norm spatial filter with recursively updated gram matrix). In the following step, the similarity between the greatest source point and entire source focuses were analyzed by a technique called coherence mapping for more exact results. Backtracking of heart structure utilizing magneto-cardiography information is in view of the figured source power from spatial filtering and coherence mapping.**

***IndexTerms*— video authentication, video encryption, Watermarking, semi fragile watermarking, Advanced video codec (AVC)**

I. INTRODUCTION

Magneto-cardiography is a non invasive technique used to determine the strength of magnetic fields that are produced by electric activity of heart. Tremendously sensitive device called superconducting quantum interference device(SQUID's). In order to overcome the drawbacks of other techniques, a novel technique is suggested which makes use of magneto-cardiography data only[11]. The current density was calculated by using non adaptive spatial filtering, particularly the minimum norm estimation. Using the integrated current density the three dimensional polygon of heart is obtained.

Here, use of array gain constraint minimum norm spatial filter with recursively updated gram matrix(AGMN-RUG) is proposed so as to improve the spatial resolution, and is based on non adaptive spatial filter. Coherence mapping method is also used in order to obtain more accurate outline/structure of heart. The results obtained from AGMN-RUG and coherence mapping are normalized by the decided thresholds on the volume comparison between the retraced outline of the atrium and ventricle and the reference.

II. METHODS

Array gain constraint minimum norm spatial filter with recursively updated gram matrix

A spatial filtering system can reproduce the cardiovascular shape, following the yield force of spatial filters can evaluate the size of myocardial electric exercises. A source vector is defined as s(r,t) at area r = (x,y,z) and time t in a discrete volume space V . The aggregate number of sources is Q. The created attractive fields from the sources measured by N-channel sensors amid time window t are meant as b(t) = [b1(t),b2(t),...,bn(t)]T where T is the grid transpose. At that point, from the sensor configuration and conductivity geometry of the source space, we can figure the affectability conveyance of sensors reacting to unit current sources. This is known as the lead-field vector and defined as l(r) ≡ [lx(r),ly(r),lz(r)], and the N×Q lead-field framework. The measurement data is obtained out of a combination of the lead-field matrix and source The spatial filter is a weight vector which is straightly increased to the deliberate attractive fields for evaluating source activities. The evaluated source vector ˆ s(r,t) is gotten from a direct blend of the weight vector, W(r), and the estimation information.

To outline a perfect spatial filter, the increase from the shaft reaction ought to be minimized. Subsequently, the base standard based spatial filter is gotten from taking care of a streamlining issue with requirements Then, the weight vector is obtained by a linear combination of the depth-normalized lead-field matrix, ˜ L(r), and the gram matrix. As the sensitivity of sensors decrease in proportion to the square of the distance, the power of superficial sources than deep sources becomes greater. As in the case of adaptive spatial filter, the minimum variance (MV) spatial filter is applied in bioelectromagnetism. The MV spatial filter is obtained from solving an optimization problem that decreases the output power under the constraint.

In order to obtain more accurate results, we have to consider the noise effects toward the gram matrix. Since the condition number, an output value of a function according to the change of an input argument, of the gram matrix in practical applications is significantly large, calculating G^{-1} generates inaccurate results. By applying the regularization method, the errors caused from calculating G^{-1} can be reduced.

Coherence mapping

Despite the fact that the heart volume is remade by utilizing the force of myocardial electrical exercises, natural commotions, for example, breath and assimilation might contrarily influence on the estimation of source force. The relationship of the spatial filtering and reasonability mapping is depicted as an applied outline in Fig. 1.

The waveforms in the source space are reproduced by duplicating the weight vector to the deliberate attractive fields. At that point the time arrangement of remade waveform is spoken to as ˆ s(rq,t) at the Qth position. Furthermore, the ˆ s(ra,t) and ˆ s(rv,t) are

waveforms at the position of maximum source power of the atrium and ventricle, separately, as demonstrated in Fig 2. As Sa(f), Sv(f), and Sq(f) are the quick Fourier changes (FFT) of ˆ s(ra,t) ˆ s(rv,t), and ˆ s(rq,t), separately, the cross-range is defined as beneath.

$$\Gamma_{aq}(f) \equiv \langle S_a(f) S_q^*(f) \rangle,$$
$$\Gamma_{vq}(f) \equiv \langle S_v(f) S_q^*(f) \rangle, \quad (1)$$

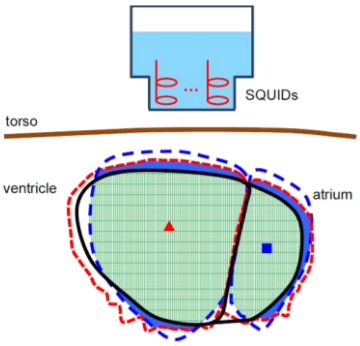

Fig. 1. An applied outline of the relationship between a spatial filtering and reasonability mapping. The (dark) strong line speaks to volumes of a simplified chamber and ventricle. The (blue) since a long time ago dashed line is reproduced volume by spatial filtering, and the (red) short dashed line is recreated volume by rationality mapping system. The thick volumes are a mix of the spatial filtering and soundness mapping system. The (green) network volume speaks to positive volume while the (blue) filled volume speaks to negative volume to the first cardiovascular volume. The (blue) rectangle and (red) triangle are the greatest source force of the chamber and ventricle, individually, and they are utilized as a turn point for calculation of coherence.

where $*$ represents the complex conjugate. Then, the coherence is defined with the absolute value of normalized crossspectrum as

$$Coh_{aq}(f) \equiv \left| \frac{\Gamma_{aq}(f)}{\sqrt{\Gamma_{aa}(f)\Gamma_{qq}(f)}} \right|,$$
$$Coh_{vq}(f) \equiv \left| \frac{\Gamma_{vq}(f)}{\sqrt{\Gamma_{vv}(f)\Gamma_{qq}(f)}} \right|. \quad (2)$$

As a rule, the length of arrived at the midpoint of MCG information is around 1000 ms to speak to one cardiovascular cycle. Be that as it may, the length of recreated waveforms for the chamber and ventricle is shorter than the found the middle value of MCG information.

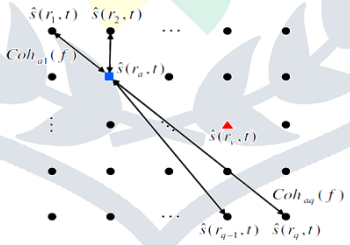

Fig. 2. An outline of the coherence mapping system by double pivot point. The projectiles are 3-D source space. The ˆ s(ra,t), and ˆ s(rv,t) are remade waveforms determined at the most extreme source force of a chamber ((blue) rectangle) and ventricle ((red) triangle) by the AGMN-Floor covering spatial filtering technique, separately. At that point, the soundness between the most extreme source point and entire source space is obtained.

III. RESULTS

Simulation experiments.

For the numerical reenactments of MCG signal, a voxel degree, source position, and source shape were created. A discretionary xiphoid position was fixed for the fiducial point. The voxel interim was 10 mm and the aggregate number was 3314 that was gotten from the point spread function. At that point, the source positions were foreordained in the 3-D space, and the distinctions in width and profundity of sources were chosen to indicate an estimate of the chamber and ventricle as seen in Fig. 3. Fig. 4 (a) portrays the produced MCG signs in view of the above conditions. Firstly, the λ was controlled by the commotion level. In this reenactment the parameter for the chamber and ventricle was situated to 0.001 and 0.0001 times to the greatest eigenvalue of every gram framework in the SNR was 20 dB. Besides, the edges of standardized source force and soundness were dead set as the volume was indistinguishable between the reproduced diagram and unique shape in view of the SNR

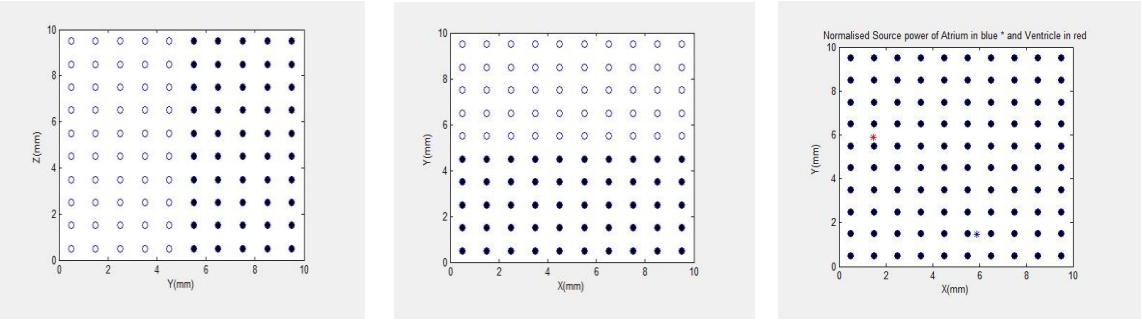

Fig. 3. Source configurations for the numerical simulation shown in the X-Y, Y-Z plane. The circle depicts an atrium and the bullet describes a ventricle.The source spacing is 10 mm. The S(ra; t), and S(rv; t) are reconstructed waveforms derived at the maximum source power of an atrium ((light blue) circle) and ventricle ((red colour triangle) by the AGMN-RUG spatial filtering method, respectively.

The consequences of numerical recreation are demonstrated in Fig. 5. The source force of chamber and ventricle were directed by the AGMN-Carpet spatial filtering system, and the standardized result is depicted in Fig. 5 (a). At that point the standardized source lucidness is delineated in Fig. 5 (b). In conclusion, the augmentation of the source force and lucidness results is likewise standardized and portrayed in Fig. 5 (c). The exactness of remade diagram was clarified by the proportion of positive and negative volume as portrayed in Fig. 1.

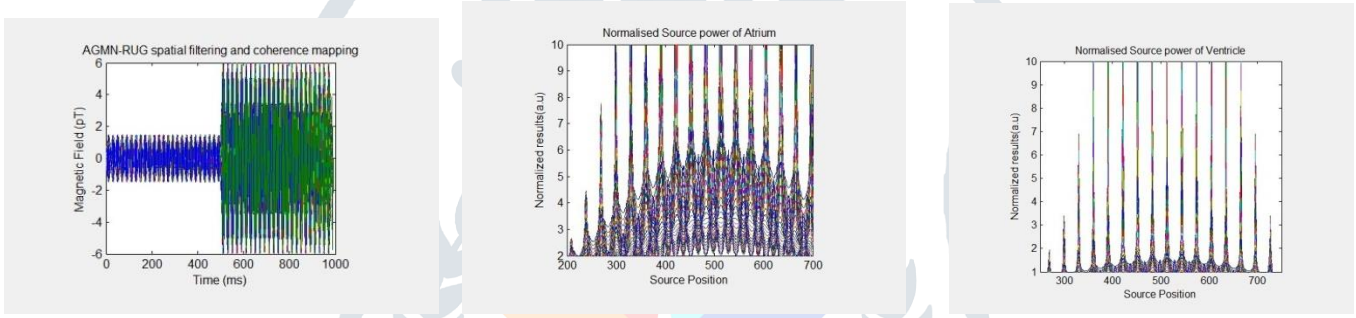

(a) (b) (c)

Fig. 4. Simulation results of the atrium and ventricle by the combination of AGMN-RUG spatial filtering and coherence mapping method, respectively. (a) Magnetic fields generated from the atrium and ventricle measured by a 64-ch MCG system. The normalized results of multiplied source power and coherence of the atrium (b) and ventricle (c).

I. DISCUSSION AND CONCLUSION

The regularization technique significantly influences on the count of source force and waveform recreation. To reconstruct the accurate cardiac blueprint, an ideal λ ought to be resolved. The choice of λ is in light of the SNR. The SNR for the reenactment is defined as SNR = 20log10(Asignal/Anoise) where An is root mean square plentifulness. This work, then again, is a first pilot approach, not explored sufficiently to judge about the execution or even to use in clinical applications.

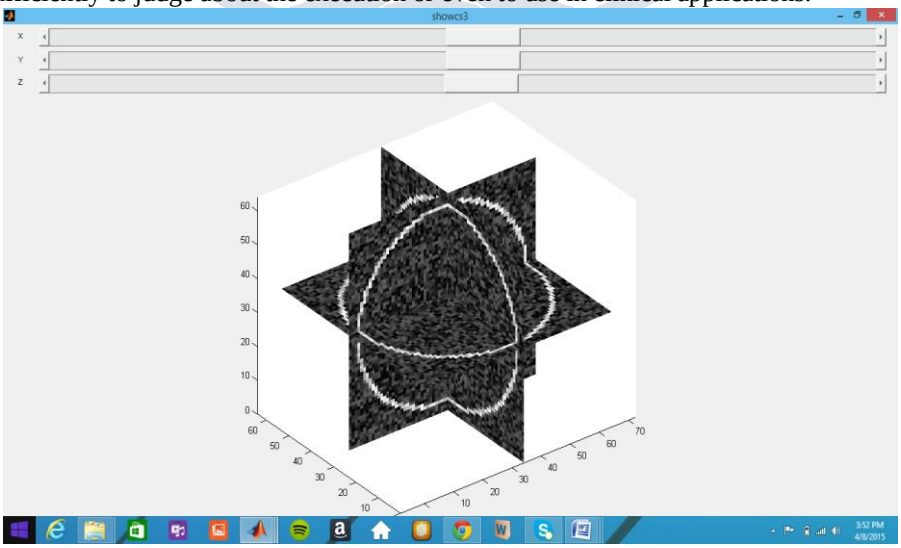

Fig. 5. Simulation results of the cardiac outline reconstruction based on threshold values for source power, coherence, and multiplication of source power and coherence by the AGMN-RUG spatial filtering and coherence mapping method. The thresholds for normalized of the atrium and ventricle for source power are 0.018 and 0.015, these for coherence are 0.041 and 0.034, and these for multiplication are 0.0058 and 0.0033.

Since the limit essentially influences the recreation of a precise heart shape, find fitting edges is compulsory before giving any evaluation on clinical estimation of this proposed technique. Consequently, we will assess the ideal limit for patients utilizing the highest level which ought to be the sensible heart and middle by CT or X-ray in significant number of human subjects.

II. ACKNOWLEDGEMENT

The authors would like to appreciate Dr.Mahesh.P.K of the Don Bosco Institute of Technology, for his kind comments on the AGMN-RUG spatial filtering method and coherence mapping method.

REFERENCES

[1] J. S. Kwong, B. Leithauser, J.-W. Park, and C.-M. Yu, "Diagnostic value of magnetocardiography in coronary artery disease and cardiac arrhythmias: A review of clinical data," International journal of cardiology, 2013.
[2] S. Haufe, V. V. Nikulin, K.-R. Muller, and G. Nolte, "A critical assessment of connectivity measures for eeg data: a simulation study," Neuroimage, 2012.
[3] K. Kim, "Source-space waveform reconstruction for coherent brain signals," in Proc. APSIPA Conf, 2011.
[4] I. Kumihashi and K. Sekihara, "Array-gain constraint minimum-norm spatial filter with recursively updated gram matrix for biomagnetic source imaging," Biomedical Engineering, IEEE Transactions on, vol. 57, no. 6, pp. 1358–1365, 2010.
[5] J. Kim, S. Kim, K. Kim, and J. Park, "Automated 3d heart segmentation by search rays for building individual conductor models," in SPIE Medical Imaging. International Society for Optics and Photonics, 2009, pp. 72611W–72611W.
[6] F. Wetterling, M. Liehr, P. Schimpf, H. Liu, and J. Haueisen, "The localization of focal heart activity via body surface potential measurements: tests in a heterogeneous torso phantom," Physics in medicine and biology, vol. 54, no. 18, p. 5395, 2009.
[7] Y. Zheng, A. Barbu, B. Georgescu, M. Scheuering, and D. Comaniciu, "Four-chamber heart modeling and automatic segmentation for 3-d cardiac ct volumes using marginal space learning and steerable features," Medical Imaging, IEEE Transactions on, vol. 27, no. 11, pp. 1668–1681, 2008.
[8] O. Ecabert, J. Peters, H. Schramm, C. Lorenz, J. von Berg, M. J. Walker, M. Vembar, M. E. Olszewski, K. Subramanyan, G. Lavi et al., "Automatic model-based segmentation of the heart in ct images," Medical Imaging, IEEE Transactions on, vol. 27, no. 9, pp. 1189–1201, 2008.
[9] K. Sekihara and S. S. Nagarajan, Adaptive spatial filters for electromagnetic brain imaging. Springer, 2008.
[10] J.-W. Park, P. M. Hill, N. Chung, P. G. Hugenholtz, and F. Jung, "Magnetocardiography predicts coronary artery disease in patients with acute chest pain," Annals of Noninvasive Electrocardiology, vol. 10, no. 3, pp. 312–323, 2005.
[11] K. Kawazoe, K. Nakai, H. Izumoto, Y. Oshima, T. Oka, J. Tsuboi, K. Yoshioka, M. Shozushima, M. Itoh, A. Suwabe et al., "Construction of a three-dimensional outline of the heart and conduction pathway by means of a 64-channel magnetocardiogram in patients with atrial flutter and fibrillation," The international journal of cardiovascular imaging, pp. 555–561, vol. 21, no. 5, 2005.
[12] D. DiPietroPaolo, H. M¨uller, and S. Ern´e, "A novel approach for the averaging of magnetocardiographically recorded heart beats," Physics in Medicine and Biology, vol. 50, no. 10, p. 2415, 2005.